Searches for leptoquarks and excited fermions at HERA

Ulrich F. Katz‡§ (ZEUS)
Representing the H1 and ZEUS Collaborations

University of Erlangen-Nuremberg, Institute of Physics,
Erwin-Rommel-Str. 1, 91058 Erlangen, Germany
Email: katz@physik.uni-erlangen.de

Abstract. Recent results on searches for new particles at the electron-proton collider HERA are reported. Based on roughly $100\,\mathrm{pb}^{-1}$ of e^+p data and $16\,\mathrm{pb}^{-1}$ of e^-p data per experiment, taken in the years 1994–2000, the H1 and ZEUS collaborations have derived new exclusion limits for the direct production of excited fermion states and leptoquarks. The latter are searched for in different decay channels, including lepton-flavor violating decays. The production of R_P-violating squarks followed by leptoquark-like decays to lepton and quark is studied, as are cascade decays yielding multi-jet plus lepton signatures. New limits from indirect searches are also reported. Several of the searches obtain sensitivities of the same order or exceeding those of other experiments, indicating the substantial discovery potential of future HERA running.

1. Introduction

From 1998 to 2000, the electron-proton collider HERA at DESY was operated with electrons or positrons at an energy of $E_e = 27.5\,\mathrm{GeV}$ and protons of $E_p = 920\,\mathrm{GeV}$, yielding a center-of-mass energy of $\sqrt{s} = 318\,\mathrm{GeV}$. In this period, the ZEUS and H1 collaborations collected e^+p (e^-p) data samples corresponding to integrated luminosities of about $66\,\mathrm{pb}^{-1}$ ($16\,\mathrm{pb}^{-1}$) per experiment. Combining these data sets with previous e^+p data at $\sqrt{s} = 300\,\mathrm{GeV}$ increases the HERA sensitivity in searches for new heavy particles to masses of almost $300\,\mathrm{GeV}$ and production cross sections as low as $0.1\,\mathrm{pb}$.

This document describes the status of searches for signals of excited fermions, leptoquarks and R_P-violating squarks. It focuses on results that include the data taken since 1998 and are thus the "last word" from HERA before the high-luminosity phase HERA-2, which is currently beginning. Earlier results have e.g. been reported at the Beyond99 conference [1]. Many of the results presented in the following are still preliminary, and some have only become available since the Beyond02 conference but are included to provide an up-to-date overview of recent experimental results. A recent review of searches at HERA and at the Tevatron is also available in [2].

2. Excited fermions

If electrons or neutrinos are composite, their excitations could be produced in ep reactions at HERA by t-channel exchange of photons, Z or W bosons as shown in
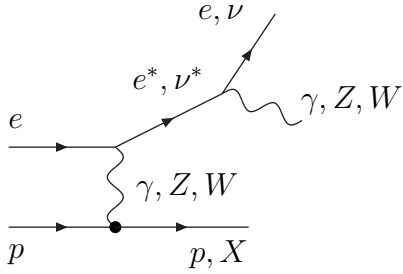
arXiv:hep-ex/0212049v1 19 Dec 2002

Figure 1. Feynman graph of the production and subsequent decay of excited electrons or neutrinos in ep reactions. In the case of e^* production, elastic reactions $ep \to e^*p$ are possible.

Table 1. Decay modes, event signatures and main SM background sources considered in the e^* and ν^* searches by H1 [3, 4] and ZEUS [5].

f^* decay	signature	main SM background	studied by
$e^* \to e + \gamma$	$e + \gamma$	QEDC, NC DIS	H1, ZEUS
$e^* \to e + Z \to e + q\bar{q}$	$e + 2\text{jets}$	NC DIS	H1
$e^* \to \nu + W \to \nu + q\bar{q}'$	$\not{P}_t + 2\text{jets}$	CC DIS, PHP	H1
$\nu^* \to \nu + \gamma$	$\gamma + \not{P}_t$	CC DIS	H1, ZEUS
$\nu^* \to \nu + Z \to \nu + q\bar{q}$	$\not{P}_t + 2\text{jets}$	CC DIS, PHP	H1, ZEUS
$\nu^* \to e + W \to e + q\bar{q}'$	$e + 2\text{jets}$	NC DIS	H1, ZEUS

the diagram of Fig. 1. The observation of such states would be a clear indication of fermion substructure.

The H1 [3, 4] and ZEUS [5, 6] collaborations have searched for excited electrons (e^*) and neutrinos (ν^*) under the assumption that they decay into standard fermions and electroweak gauge bosons in one of the modes summarized in Table 1. Whereas e^* production is expected to occur in e^+p and e^-p reactions with about the same cross section, ν^* would be produced in e^-p scattering at a much higher rate than in e^+p reactions, so the ν^* searches focus on the e^-p data. The main selection cuts for both the e^* and ν^* searches required events consistent with the presence of both a final-state lepton with high transverse momentum, P_t (either an electron identified in the central detector or large missing transverse momentum, $\not{P}_t$, indicating a neutrino) and of the gauge boson from the f^* decay (either identified directly in the case of a photon, or via the hadronic decay products in the case of W and Z bosons). The backgrounds from various Standard Model (SM) processes (mainly neutral current (NC) and charged current (CC) deep-inelastic scattering (DIS), QED Compton scattering (QEDC) and photoproduction of jets with high transverse momentum (PHP), see Table 1) are estimated from MC simulations. The signal reactions are simulated using cross sections calculated according to the model by Hagiwara, Zeppenfeld and Komamiya (HZK) [7] for spin-1/2 excited fermions.

No indication of a signal above SM background has been found. As an example, Fig. 2 shows the distribution of the invariant $e\gamma$ mass in the event sample selected in the ZEUS search for $e^* \to e\gamma$ decays, together with the expected signal shape for an e^* with $M_{e^*} = 225\,\text{GeV}$ (arbitrary normalization). For excited fermion (f^*) masses $M_{f^*} \gtrsim 100\,\text{GeV}$ the searches are almost background-free, yielding upper limits at 95% C.L. on the cross section times branching ratio ($\sigma \cdot \text{BR}$) of typically $0.05-0.1\,\text{pb}$ for the decay channels with highest sensitivity.

The HZK model is used to relate these limits to exclusion plots of f/Λ vs. M_{f^*}, where Λ is the characteristic mass scale and f denotes the coupling at the f^*-fermion-boson vertex. In the HZK model, there are three independent couplings, of which that to gluons (f_s) is irrelevant for e^* and ν^* production at HERA and those to the U(1) (f')
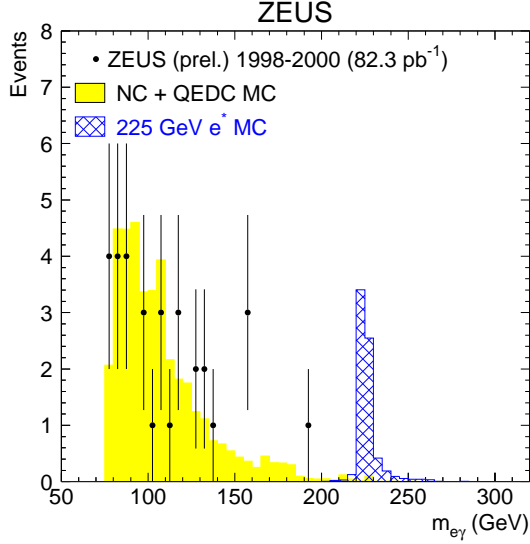
Figure 2. Spectrum of the invariant $e\gamma$ mass of ZEUS candidates for e^* production and subsequent decay $e^* \rightarrow e\gamma$. The points with error bars show the data and the light-shaded histogram the total SM background. The hatched histogram illustrates the signal expected for a hypothetical e^* with a mass of 225 GeV.

and SU(2) (f) gauge fields are either assumed to be related by $f = \pm f'$, or their ratio is varied in the range $|f'/f| \leq 5$ (H1). The ratio $|f'/f|$ fixes the relative contributions of photon and Z exchange in e^* production and also the branching ratios of the f^* decays for a given M_{f^*}. The resulting exclusion limits on f/Λ for e^* are compared to the corresponding LEP results [8] in Fig. 3. Also shown is the dependence of these limits on f'/f. For $f = -f'$, the e^* has no electromagnetic interactions and hence must be produced by Z exchange and in addition does not decay to $e\gamma$, thus reducing the HERA sensitivity substantially. Figure 4 shows the exclusion limits for ν^* from the H1 analysis, together with a recent L3 result [9]; similar results are obtained by ZEUS (not shown). The dependence on f'/f is weaker than in the e^* case since ν^* production requires the
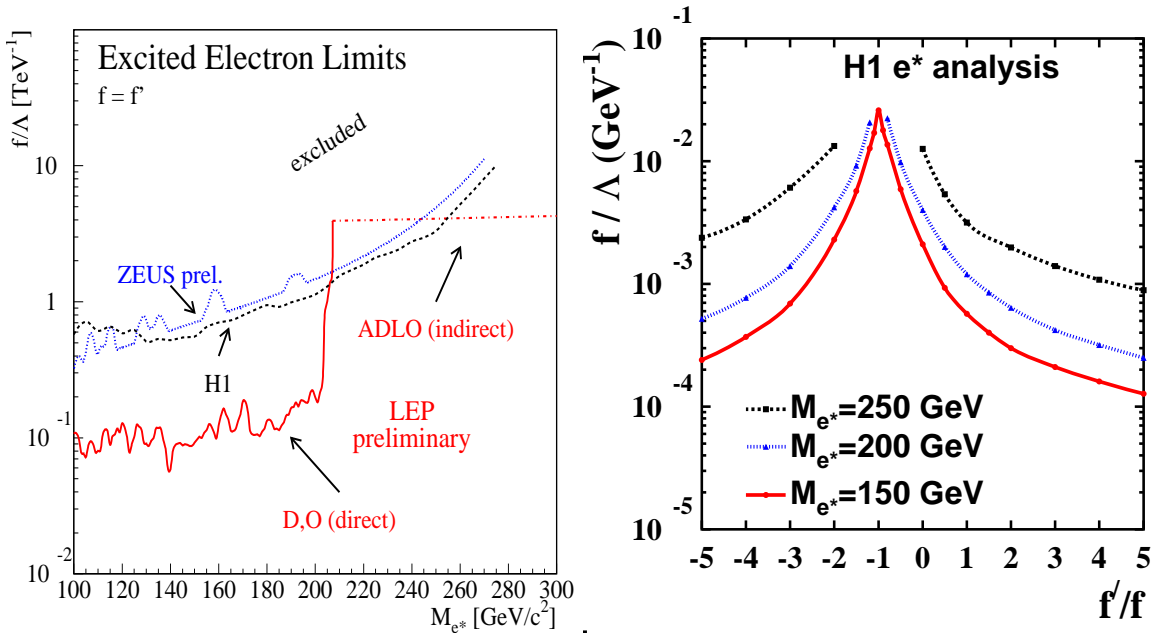

Figure 3. Left: limits at 95% C.L. on f/Λ from the H1 and ZEUS searches for excited electrons compared to corresponding results from the LEP experiments. Right: dependence of the H1 limits on the ratio f'/f.
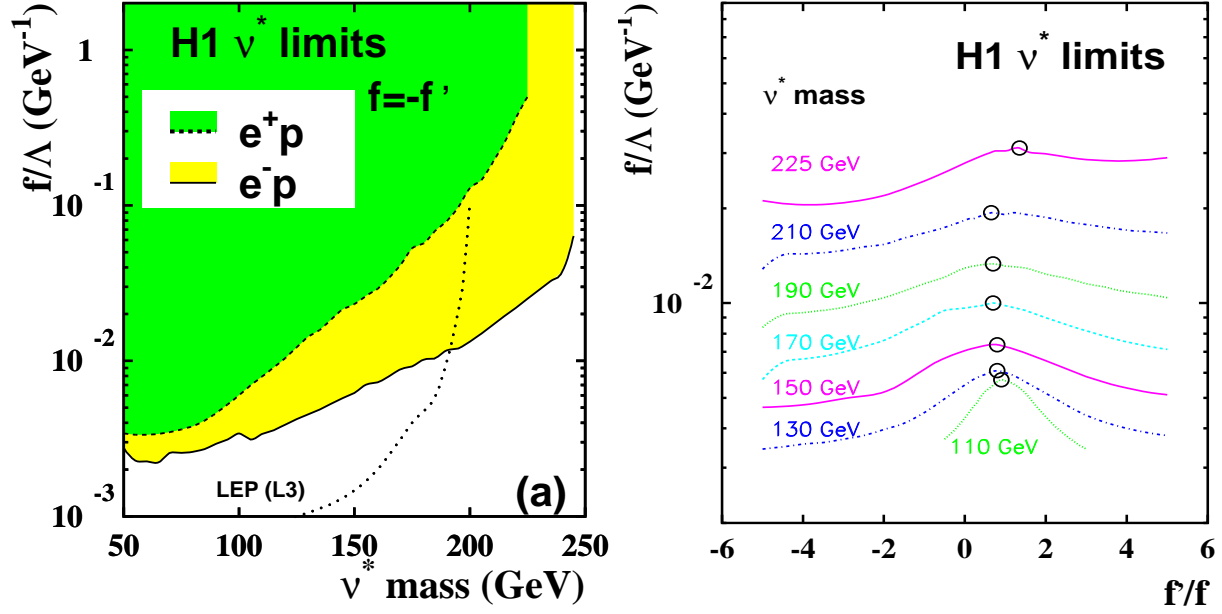
Figure 4. Left: limits at 95% C.L. on f/Λ from the H1 search for excited neutrinos compared to a corresponding result from L3. Right: dependence of the H1 limits on the ratio f'/f.

exchange of a W boson. Minimal sensitivity is obtained around $f = f'$, where the decay $\nu^* \to \nu\gamma$ is prohibited.

Assuming $f/\Lambda = 1/M_{f^*}$, the results exclude at 95% C.L. the existence of e^* with masses between 100 and about 255 GeV for $f' = f$ (estimated from Fig. 3), and of ν^* between 100 and 135(158) GeV for $f' = -f$ ($f' = f$) [5].

The HERA limits shown in Figs. 3 and 4 are weaker than the LEP limits for f^* masses below about 200 GeV, where e^* and ν^* could be directly produced in reactions of the type $e^+e^- \to f f^*$. For higher e^* masses, the LEP sensitivity comes from cross section deviations from the SM expectation for the reaction $e^+e^- \to \gamma\gamma$ which would be induced by t-channel exchange of an e^*; in this region, the HERA and LEP limits are of similar magnitude, indicating substantial discovery potential in future high-luminosity HERA running.

3. Direct searches for leptoquarks and R_P-violating squarks

Leptoquarks (LQs) are hypothesized bosons coupling to lepton-quark pairs. They could be resonantly produced in ep reactions according to the diagram of Fig. 5. Buchmüller, Rückl and Wyler (BRW) [10] have classified LQs which (i) conserve the SM gauge symmetries, (ii) only couple to quarks, leptons and SM gauge bosons and (iii) only have flavor-diagonal couplings, in ten different states characterized by their fermion number ($|F|=2$ or $F=0$), spin (scalar (S) or vector (V)) and weak isospin. Premise (ii) implies
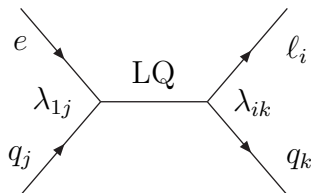

Figure 5. Feynman graph of the resonant production of an $F=2$ LQ in electron-quark scattering. The subscripts of the Yukawa couplings at the production and decay vertices of the LQ indicate the generations of the leptons and quarks involved.

that LQs only decay into $\ell^{\pm}q$ or $\nu q'$ pairs with given branching ratios. In many recent LQ searches, this assumption is dropped and a variable branching ratio $\beta_{\ell} = \mathrm{BR}(\mathrm{LQ} \to \ell^{\pm}q)$ is assigned to the LQs (accounting e.g. for the case of R_P-violating squarks).

3.1. First-generation leptoquarks

LQs coupling only to first-generation leptons can be produced at HERA in reactions of the type $ep \to \mathrm{LQ} + X \to eq + X \ (\nu_e q' + X)$, yielding the same event topologies as NC (CC) DIS at high eq invariant mass. The distinctive LQ signature is a resonant peak in the $\sqrt{xs}$ distribution around the LQ mass, M_{LQ}, where $\sqrt{s}$ is the ep center-
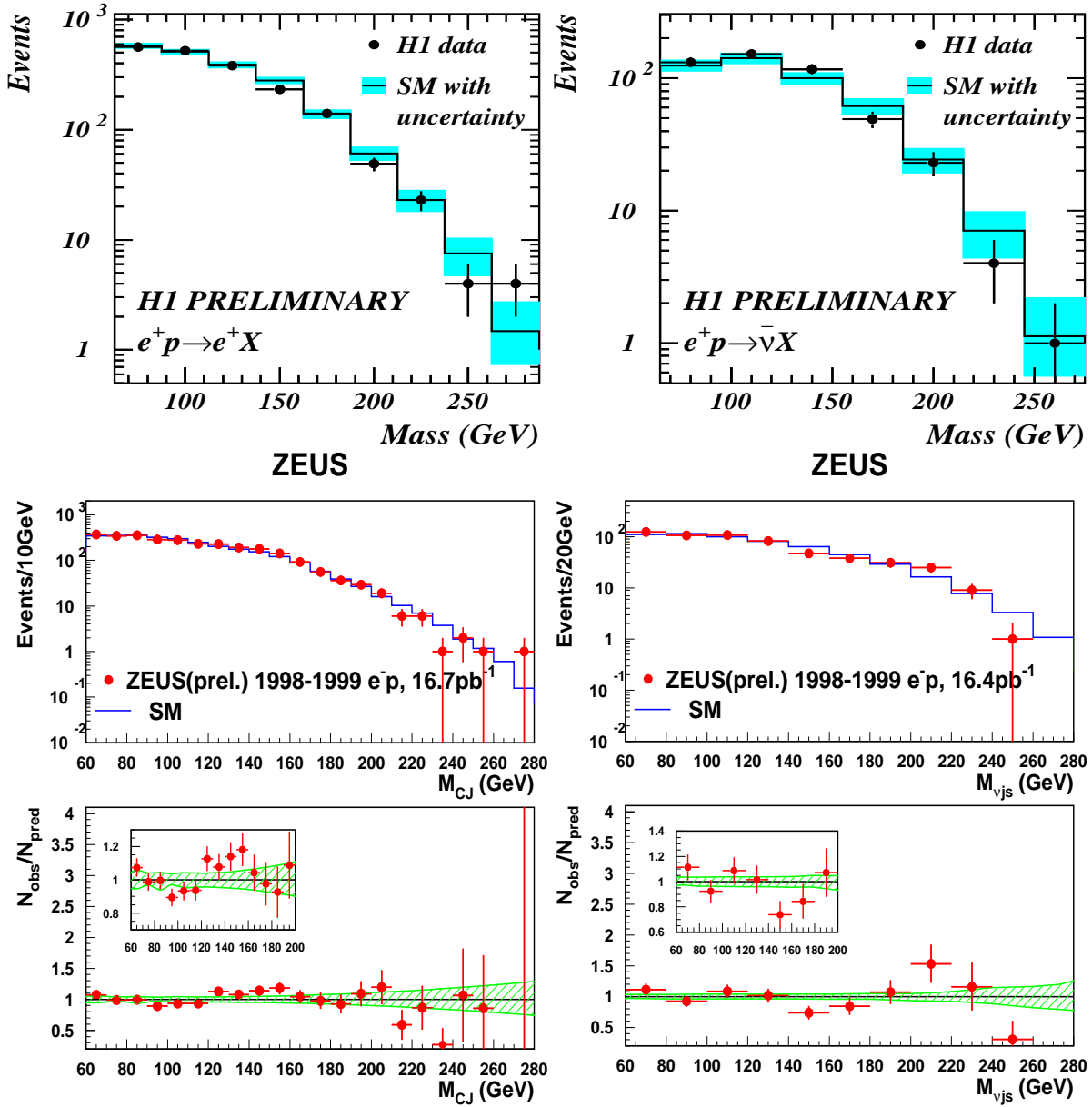

Figure 6. Distributions of the reconstructed mass $M = \sqrt{xs}$ for the H1 e^+p data (top [11]) and the ZEUS e^-p data (bottom [12]). The left column shows the NC, the right column the CC data sets. The symbols with statistical error bars represent the data, the histograms the DIS simulation. The shaded areas indicate the uncertainties of the SM predictions.

of-mass energy and the Bjorken variable, x, is the fraction of the proton momentum carried by the struck quark. Furthermore, the LQ decay angular distribution implies harder distributions in $y = s/(xQ^2)$ than for DIS (Q^2 is the negative square of the four-momentum transfer between e and p). LQ production at HERA received particular attention after H1 [13] and ZEUS [14] reported an excess of events of NC DIS at high x and Q^2 in their 1994–1996 data.

ZEUS [12] and H1 [11, 16] have searched in the available DIS data for deviations from the SM prediction consistent with a LQ signal. The data agree well with the SM and show no sign of LQ production. The previously reported event excess has not been confirmed by the new high-statistics data. As representative examples, the distributions of the reconstructed mass $M = \sqrt{xs}$ are shown in Fig. 6 for the H1 e^+p data (top) and the ZEUS e^-p data (bottom). In the NC channel ($ep \to eX$), H1 derives M from the
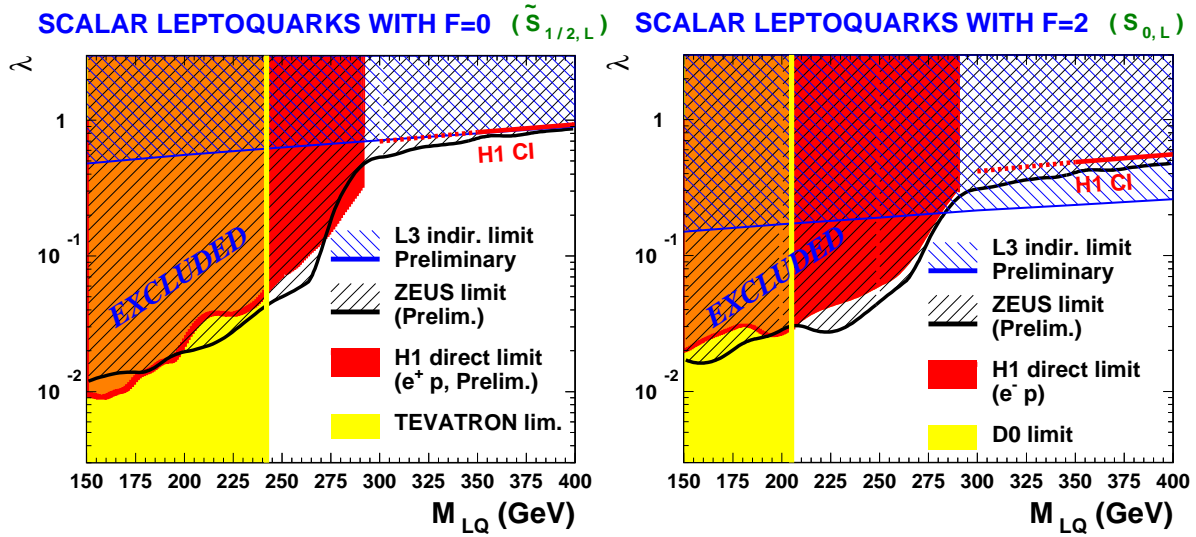

Figure 7. ZEUS and H1 exclusion limits at 95% C.L. on the LQ Yukawa coupling $\lambda = \lambda_{11}$ as a function of the LQ mass for two representative scalar LQ species, $\tilde{S}_{1/2,L}$ (left) and $S_{0,L}$ (right). Also shown are the results from indirect searches at LEP (L3) and the search for LQ pair production at the Tevatron.

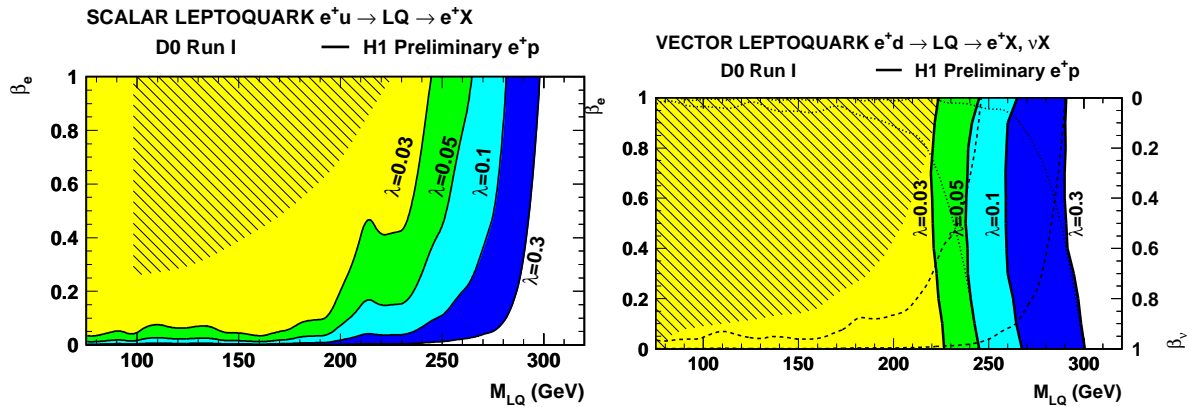**Figure 8.** H1 exclusion limits on β_e as a function of M_{LQ} for different assumptions on λ, for a scalar LQ coupling to e^+u (left) and for a vector LQ coupling both to e^+d and $\bar{\nu}u$ (right). In the right plot, the exclusion limits obtained from the NC and CC channels alone are indicated by dashed and dotted lines, respectively. The hatched areas denote the regions excluded by DØ [15].

energy and angle of the scattered electron, whereas ZEUS uses the electron energy and the kinematic variables of hadronic jets with transverse momentum exceeding $15\,\mathrm{GeV}$. For CC reactions ($ep \to \overset{(-)}{\nu} X$), H1 reconstructs M from the energy, longitudinal and transverse momentum of the hadronic final state, whereas ZEUS derives M as the invariant mass of the reconstructed neutrino and the jets with a transverse momentum above $10\,\mathrm{GeV}$.

In the absence of a LQ signal, exclusion limits on the Yukawa coupling, $\lambda = \lambda_{11}$, are derived as a function of M_{LQ} for LQs coupling to first-generation quarks and leptons ($i = j = k = 1$ in Fig. 5). This analysis is based on the BRW model. The results are shown in Fig. 7 for two representative scalar LQ species with $|F|=2$ and $F=0$, respectively. In order to set limits, the event distributions in M and y are compared to MC simulations of DIS reactions and of signal events. For LQs that can decay both to eq and $\nu q'$, the limits are inferred from the NC and CC data sets. Taking into account u-channel LQ exchange and the DIS-LQ interference, in addition to the s-channel LQ formation of Fig. 5 (which dominates for $M_{\mathrm{LQ}} \lesssim 240\,\mathrm{GeV}$), yields sensitivity to LQ masses up to and beyond the HERA center-of-mass energy (ZEUS). Alternatively, a contact interaction approach (see Sect. 4) can be used to constrain high-mass LQs (H1). Note that the sensitivity is highest for LQs that can be produced from valence quarks, i.e. for LQs with $F=0$ in e^+p and for LQs with $F=2$ in e^-p scattering. Also indicated in Fig. 7 are the exclusion limits obtained by L3 [17] (from a search for anomalous contributions to the cross section $\sigma(e^+e^- \to \text{hadrons})$ induced by the t-channel exchange of LQs) and from the Tevatron, where LQs could be pair-produced with a rate that is independent of λ. The combined CDF and DØ limit is $M_{\mathrm{LQ}} > 242\,\mathrm{GeV}$ [18] for scalar LQs with $\beta_e = 1$ and is expected to be even higher for vector LQs.

H1 has derived LQ exclusion limits as functions of β_e and M_{LQ} for fixed values of λ [11] (Fig. 8), thus allowing a direct comparison to the LQ exclusion region from DØ [15]. Figures 7 and 8 demonstrate that the HERA experiments have a unique discovery potential for LQs with low β_e and masses beyond about $200\,\mathrm{GeV}$.

3.2. R_P-violating squarks

In supersymmetric models without conservation of R-parity, $R_P = (-1)^{3B+L+2S}$ (B being the baryon number, L the lepton number and S the spin), squarks can have Yukawa couplings λ'_{ijk} to leptons and quarks and thus behave like LQs (see [19, 20] and references therein). The generation indices are $i = 1$ for the electron, j for the squark and k for the quark. The dominant production cross section, and thus the highest sensitivity at HERA, is expected for $\tilde{u}$-type squarks which can be produced from d quarks, whereas all other squarks couple only to the quark sea in the proton. The searches at HERA focus on this scenario, assuming that one coupling λ'_{1j1} is non-zero and other flavor combinations do not contribute to the cross section.

In addition to the LQ-like decay $\tilde{q}_j \to ed$, squarks can also undergo cascade gauge decays, with R_P-violating processes occuring further down the chain. Examples for such cascades are shown in Fig. 9. These reactions produce events with distinctive signatures: several jets and one or more leptons with high transverse momentum, where in some channels the final-state electron can have opposite charge to that of the beam electron. Using about $40\,\mathrm{pb}^{-1}$ of e^+p data collected in 1994–97, ZEUS [21] and H1 [22] have searched for squark production in e^+p scattering by combining the results of the LQ analyses in the NC channel (squarks cannot decay to $\overset{(-)}{\nu} q$) with dedicated searches for events that are consistent with squark cascade decays. No significant excess over the SM background was found, and exclusion limits on λ'_{1j1} as a function of the squark mass
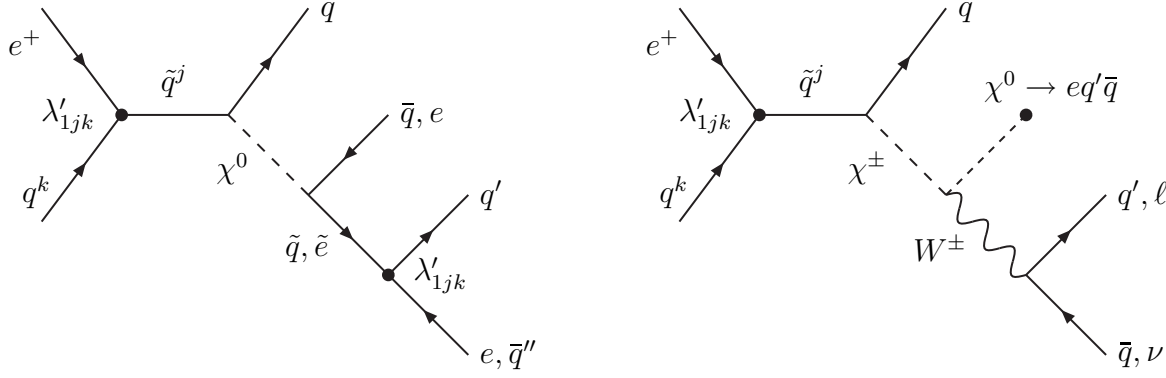
Figure 9. Examples for cascade decays of squarks in R_P-violating supersymmetry. The R_P-violating vertices are marked with dots. The symbols χ^0 and $\chi^\pm$ denote the neutralino and the chargino, respectively.
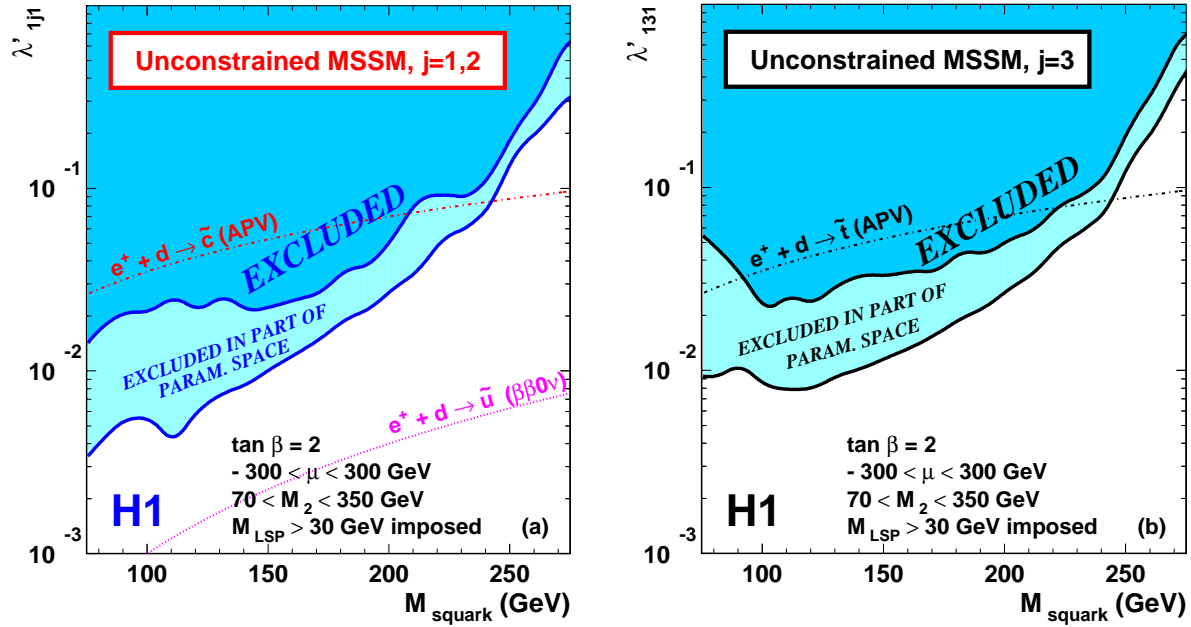

Figure 10. H1 exclusion limits on λ'_{1j1} as a function of the squark mass for $\tilde{u}$ and $\tilde{c}$ squarks ($j = 1, 2$, left) and for $\tilde{t}$ squarks ($j = 3$, right). For fixed $\tan\beta$, the supersymmetric parameters μ and M_2 have been scanned in the ranges indicated on the plots. The dark shaded region is excluded for all parameter combinations, whereas the light shaded region is excluded only in part of the parameter space. The dotted and dash-dotted lines indicate the exclusion limits from low-energy measurements [19].

have been set. The H1 results are shown in Fig. 10. It can be seen that for $j = 2, 3$ the sensitivity of HERA greatly exceeds that of the currently most sensitive low-energy probe, atomic parity violation (APV); for $j = 1$, however, the limits obtained from neutrinoless double-beta decay are much stronger than those from HERA [19].

3.3. Lepton-flavor violating leptoquarks

Leptoquarks or squarks that couple to leptons of several generations simultaneously (i.e. $\lambda_{1j} \neq 0$ and $\lambda_{ik} \neq 0$ for at least one flavor combination with $i > 1$, see Fig. 5) could induce lepton-flavor violating (LFV) DIS-like reactions at HERA with the final-state e
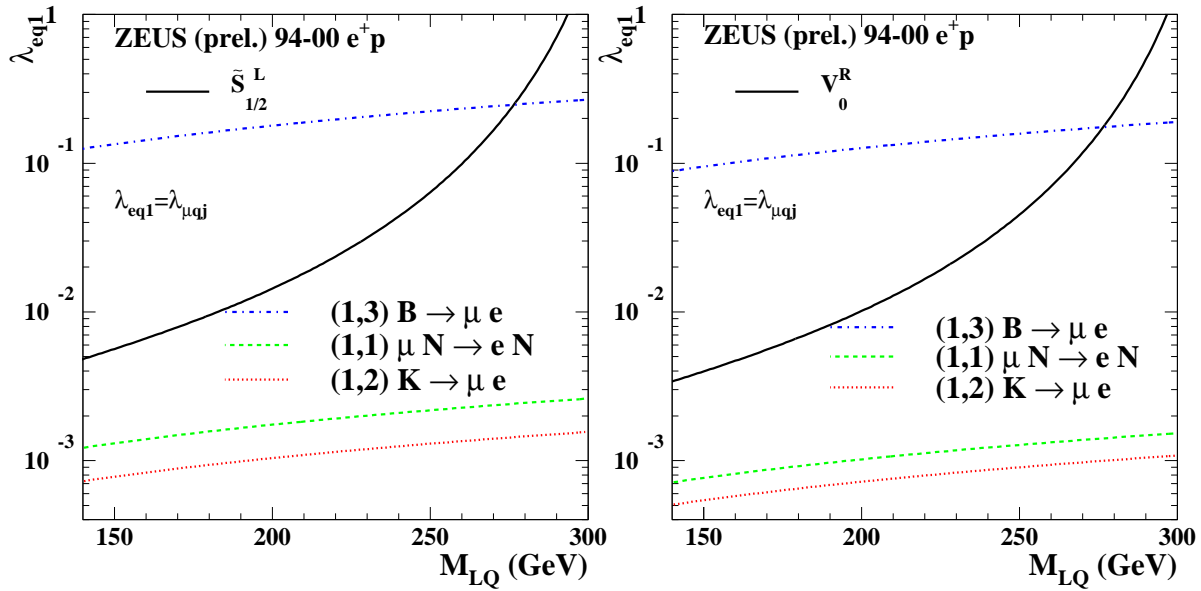
Figure 11. ZEUS exclusion limits at 95% C.L. on the coupling strength λ_{2k} of LFV LQs under the assumption $\lambda_{2k} = \lambda_{11}$. The limits are shown for scalar (left) and vector (right) LQ species that couple to d quarks and thus yield minimal sensitivity in the ZEUS search. Also shown are the limits from rare processes [26], where the numbers in parentheses indicate the quark generations that couple to the e and the μ, respectively.

replaced by a μ or τ. Searches for such events in the 1994–97 e^+p data by ZEUS [23] and H1 [24], as well as an update by ZEUS for the μ channel based on the full e^+p data sample [25], yielded no evidence for LFV. The exclusion limits [25] for the LQ couplings resulting under the assumption $\lambda_{11} = \lambda_{2k}$ (i.e. BR(LQ $\rightarrow \mu q_k$) = 1/2) are shown in Fig. 11. Assuming couplings of electromagnetic strength, $\lambda_{11} = \lambda_{2k} = \sqrt{4\pi\alpha}$, these limits correspond to $M_{\mathrm{LQ}} > 279$–$301\,\mathrm{GeV}$, depending on the LQ type. Comparison of the ZEUS results with limits derived from searches for low-energy rare processes [26] (see Fig. 11) shows that the HERA data are highly sensitive to LFV LQs coupling to 3rd-generation quarks but less so if $k = 1$ or if q_k is a s quark. The Tevatron experiments report mass limits on LQs decaying to μq or τq (see [2] and references therein), but since LQs would be pair-produced in $p\bar{p}$ reactions via QCD gauge couplings, these results do not constrain LFV.

4. Indirect leptoquark and squark searches

As mentioned in Sect. 3.1, LQs and squarks coupling to electrons and quarks affect the ep DIS cross section through virtual u- and s-channel exchange, even if their masses exceed the HERA center-of-mass energy; note that in this case the characteristic resonance-like signal in xs disappears. The search for such high-mass signatures is usually performed using a contact interaction approach, which parameterizes the cross section modification in terms of a global mass scale, Λ, and of sets of chiral couplings of the hypothesized heavy object to the different quark flavors. The results of such analyses have been provided by ZEUS [27, 28] and H1 [29, 30]. For the special case of LQs conforming to the BRW model, the contact interaction limits can be converted to lower bounds on M_{LQ}/λ. Figure 12 shows the ratio of measured to predicted Q^2 distributions in the ZEUS e^+p and e^-p NC data together with the expected modifications induced by scalar LQs; these lines correspond to the 95% C.L. lower limit on M_{LQ}/λ. Note the
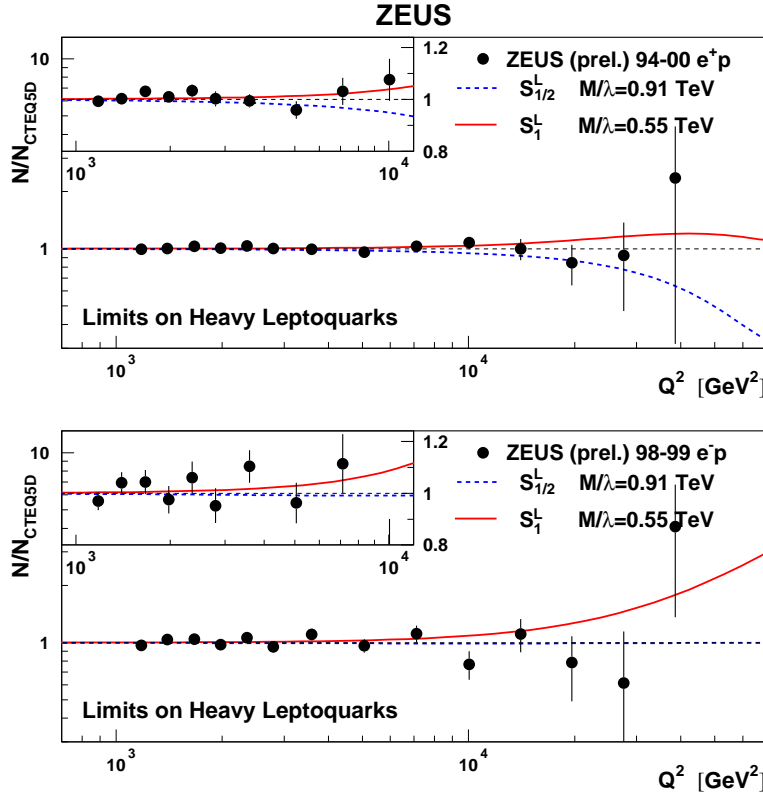
Figure 12. Ratios of measured to predicted Q^2 distributions in the ZEUS e^+p (top) and e^-p (bottom) NC data. The solid (dotted) lines show the expected modifications induced by S_1^L ($S_{1/2}^L$) LQs with M_{LQ}/λ corresponding to the 95% C.L. lower limit.

LQ or $\tilde{q}$	F	$M_{\mathrm{LQ}}/\lambda\,[\mathrm{GeV}]$		LQ or $\tilde{q}$	F	$M_{\mathrm{LQ}}/\lambda\,[\mathrm{GeV}]$	
		ZEUS	H1			ZEUS	H1
S_0^L or $\tilde{d}$	2	750	720	V_0^L	0	690	770
S_0^R	2	690	670	V_0^R	0	580	640
$\tilde{S}_0^R$	2	310	330	$\tilde{V}_0^R$	0	1030	1000
S_1^L	2	550	480	V_1^L	0	1420	1380
$S_{1/2}^L$	0	910	870	$V_{1/2}^L$	2	490	420
$S_{1/2}^R$	0	690	370	$V_{1/2}^R$	2	1150	940
$\tilde{S}_{1/2}^L$ or $\tilde{u}$	0	500	430	$\tilde{V}_{1/2}^L$	2	1260	1020

Table 2. Lower limits at 95% C.L. on M_{LQ}/λ for the BRW LQ species derived by the contact interaction analyses of ZEUS [28] and H1 [30]. Note that with $\lambda \equiv \lambda'_{1j1}$ the limits for the scalar LQs S_0^L and $\tilde{S}_{1/2}^L$ also apply to $\tilde{d}$- and $\tilde{u}$-type squarks, respectively

complementary sensitivity of the data sets to the different LQ species. The M_{LQ}/λ limits for all BRW LQ species and for $\tilde{u}$- and $\tilde{d}$-type R_P-violating squarks as obtained by ZEUS [28] and H1 [30] are summarized in Table 2. The assumptions implicit in the contact interaction approach restrict the applicability of these results to high-mass LQs, i.e. to $M_{\mathrm{LQ}} \gg \sqrt{s} = 318\,\mathrm{GeV}$. As is also seen in Fig. 7, these limits are weaker than those from the direct search but still restrictive for LQ masses up to a few TeV.

High-mass exclusion limits for the combination $\lambda_{1j}\lambda_{ik}/M_{\mathrm{LQ}}^2$ characterizing LFV LQs can be derived in a manner similar to that used for the first-generation LQs. From the absence of LFV signal events (which are very similar to those of the direct search) in the μ channel, ZEUS [25] infers upper limit values on $\lambda_{1j}\lambda_{2k}/M_{\mathrm{LQ}}^2$ for the various combinations of j, k and LQ species. The results for LQs with $F{=}0$ are shown in Table 3, the limits for $F{=}2$ are of equal magnitude. Some of these limits are stronger than those from other measurements. This also applies for similar results published previously by ZEUS [23] and H1 [24] for the τ channel.

Table 3. ZEUS [25] 95% C.L. upper limits on $\lambda_{1\alpha}\lambda_{2\beta}/M_{\mathrm{LQ}}^2$ in units of TeV^{-2}, for LQs with $F{=}0$ that couple to eq_α and to μq_β. Each cell of the table shows, from top to bottom, the reaction or decay yielding the most restrictive low-energy constraint [26], the corresponding limit and the ZEUS result (enclosed in a box when stronger than the low-energy limit). Stars (*) indicate cases involving a top quark.

	$e \to \mu$			ZEUS (prel.) ep 94-00			$F=0$
$\alpha\beta$	$S_{1/2}^L$ e^+u_α	$S_{1/2}^R$ $e^+(u+d)_\alpha$	$\tilde{S}_{1/2}^L$ e^+d_α	V_0^L e^+d_α	V_0^R e^+d_α	$\tilde{V}_0^R$ e^+u_α	V_1^L $e^+(\sqrt{2}u+d)_\alpha$
1 1	$\mu N \to eN$ 7.6×10^{-5} 1.1	$\mu N \to eN$ 2.6×10^{-5} 0.9	$\mu N \to eN$ 7.6×10^{-5} 1.6	$\mu N \to eN$ 2.6×10^{-5} 1.0	$\mu N \to eN$ 2.6×10^{-5} 1.0	$\mu N \to eN$ 2.6×10^{-5} 0.8	$\mu N \to eN$ 1.1×10^{-5} 0.4
1 2	$D \to \mu\bar{e}$ 4 $\boxed{1.2}$	$K \to \mu\bar{e}$ 2.7×10^{-5} 1.0	$K \to \mu\bar{e}$ 2.7×10^{-5} 1.7	$K \to \mu\bar{e}$ 1.3×10^{-5} 1.2	$K \to \mu\bar{e}$ 1.3×10^{-5} 1.2	$D \to \mu\bar{e}$ 2 $\boxed{1.0}$	$K \to \mu\bar{e}$ 1.3×10^{-5} 0.5
1 3	*	$B \to \mu\bar{e}$ 0.8 1.8	$B \to \mu\bar{e}$ 0.8 1.8	V_{ub} 0.2 1.5	$B \to \mu\bar{e}$ 0.4 1.5	*	V_{ub} 0.2 1.5
2 1	$D \to \mu\bar{e}$ 4 $\boxed{3.6}$	$K \to \mu\bar{e}$ 2.7×10^{-5} 2.4	$K \to \mu\bar{e}$ 2.7×10^{-5} 3.2	$K \to \mu\bar{e}$ 1.3×10^{-5} 1.3	$K \to \mu\bar{e}$ 1.3×10^{-5} 1.3	$D \to \mu\bar{e}$ 2 $\boxed{1.3}$	$K \to \mu\bar{e}$ 1.3×10^{-5} 0.6
2 2	$\mu \to ee\bar{e}$ 5×10^{-3} 5.8	$\mu \to ee\bar{e}$ 7.3×10^{-3} 3.1	$\mu \to ee\bar{e}$ 1.6×10^{-2} 3.8	$\mu \to ee\bar{e}$ 8×10^{-3} 1.9	$\mu \to ee\bar{e}$ 8×10^{-3} 1.9	$\mu \to ee\bar{e}$ 2.5×10^{-3} 2.9	$\mu \to ee\bar{e}$ 1.5×10^{-3} 1.2
2 3	*	$B \to \bar{\mu}eK$ 0.6 4.3	$B \to \bar{\mu}eK$ 0.6 4.3	$B \to \bar{\mu}eK$ 0.3 2.9	$B \to \bar{\mu}eK$ 0.3 2.9	*	$B \to \bar{\mu}eK$ 0.3 2.9
3 1	*	$B \to \mu\bar{e}$ 0.8 4.4	$B \to \mu\bar{e}$ 0.8 4.4	V_{ub} 0.2 1.5	$B \to \mu\bar{e}$ 0.4 1.5	*	V_{ub} 0.2 1.5
3 2	*	$B \to \bar{\mu}eK$ 0.6 5.8	$B \to \bar{\mu}eK$ 0.6 5.8	$B \to \bar{\mu}eK$ 0.3 2.2	$B \to \bar{\mu}eK$ 0.3 2.2	*	$B \to \bar{\mu}eK$ 0.3 2.2
3 3	*	$\mu \to ee\bar{e}$ 7.3×10^{-3} 7.7	$\mu \to ee\bar{e}$ 1.6×10^{-2} 7.7	$\mu \to ee\bar{e}$ 8×10^{-3} 3.9	$\mu \to ee\bar{e}$ 8×10^{-3} 3.9	*	$\mu \to ee\bar{e}$ 1.5×10^{-3} 3.9

References

[1] U.F. Katz, Proc. *Beyond the Desert 1999*, H.V. Klapdor-Kleingrothaus, I.V. Krivosheina (ed.), p. 671, IOP, Bristol, UK (1999). Also in preprint hep-ex/9910012.

[2] M. Kuze, Y. Sirois, preprint DESY-02-165 (hep-ex/0211048), DESY, 2002.

[3] H1 Coll., C. Adloff et al., Phys. Lett. **B 525**, 9 (2002).

[4] H1 Coll., C. Adloff et al., Phys. Lett. **B 548**, 35 (2002).

[5] ZEUS Coll., S. Chekanov et al., preprint DESY-01-132 (hep-ex-0109018), DESY, 2001; ZEUS Coll., Abstract 607, EPS-HEP, Budapest, July 12–18, 2001, available from `http://www-zeus.desy.de/physics/phch/conf/eps01_paper.html`.

[6] ZEUS Coll., available from `http://www-zeus.desy.de/physics/exo/ZEUS_PUBLIC/exo_public.html`.

[7] K. Hagiwara, D. Zeppenfeld and S. Komamiya, Z. Phys. **C 29**, 115 (1985).

[8] LEP Exotica Working Group, available from `http://lepexotica.web.cern.ch/LEPEXOTICA`.

[9] L3 Coll., M. Acciarri et al., Phys. Lett. **B 502**, 37 (2001).

[10] W. Buchmüller, R. Rückl and D. Wyler, Phys. Lett. **B 191**, 442 (1987). Erratum Phys. Lett. **B 448**, 320 (1999).

[11] H1 Coll., Abstract 1027, ICHEP, Amsterdam, July 24–31, 2002, available from `http://www.ichep02.nl/Paper/ABS1027.21aW6g.ps`.

[12] ZEUS Coll., Abstract 907, ICHEP, Amsterdam, July 24–31, 2002, available from `http://www.ichep02.nl/Paper/ABS907.200l9h.ps`.

[13] H1 Coll., C. Adloff et al., Z. Phys. **C 74**, 191 (1997).

[14] ZEUS Coll., J. Breitweg et al., Z. Phys. **C 74**, 207 (1997).

[15] DØ Coll., B. Abbott et al., Phys. Rev. Lett. **80**, 2051 (1998); DØ Coll., B. Abbott et al., Phys. Rev. Lett. **79**, 4321 (1997).

[16] H1 Coll., C. Adloff et al., Phys. Lett. **B 523**, 234 (2001).

[17] L3 Coll., Abstract 462, ICHEP, Amsterdam, July 24–31, 2002, L3 note 2759, available from `http://www.ichep02.nl/Paper/ABS462.756V9E.ps`.

[18] CDF and DØ Colls., C. Grosso-Pilcher et al., preprint FERMILAB–PUB–98–312–E (hep-ex/9810015), Fermilab, 1998.

[19] H. Dreiner, *An introduction to explicit R-parity violation*, in *Perspectives on Supersymmetry*, ed. G.L. Kane, p. 462. World Scientific, Singapore, 1998. Also in hep-ph/9707435.

[20] U.F. Katz, *Deep-Inelastic Positron–Proton Scattering in the High-Momentum-Transfer Regime of HERA*, Springer Tracts in Modern Physics, Vol. 168. Springer, Berlin, Heidelberg, 2000.

[21] ZEUS Coll., Abstract 1042, ICHEP, Osaka, July 27–August 2, 2000, available from `http://www-zeus.desy.de/physics/phch/conf/osaka_paper.html`.

[22] H1 Coll., C. Adloff et al., Eur. Phys. J. **C 20**, 639 (2001).

[23] ZEUS Coll., S. Chekanov et al., Phys. Rev. **D 65**, 092004 (2002).

[24] H1 Coll., C. Adloff et al., Eur. Phys. J. **C 11**, 447 (1999). Erratum Eur. Phys. J. **C 14**, 553 (2000).

[25] ZEUS Coll., Abstract 906, ICHEP, Amsterdam, July 24–31, 2002, available from `http://www.ichep02.nl/Paper/ABS906.63S6sE.ps`.

[26] S. Davidson, D. Bailey and B.A. Campbell, Z. Phys. **C 61**, 613 (1994); E. Gabrielli, Phys. Rev. **D 62**, 055009 (2000); Particle Data Group, K. Hagiwara et al., Phys. Rev. **D 66**, 010001 (2002).

[27] ZEUS Coll., J. Breitweg et al., Eur. Phys. J. **C 14**, 239 (2000).

[28] ZEUS Coll., Abstract 602, EPS-HEP, Budapest, July 12–18, 2001, available from `http://www-zeus.desy.de/physics/phch/conf/eps01_paper.html`.

[29] H1 Coll., C. Adloff et al., Phys. Lett. **B 479**, 358 (2000).

[30] H1 Coll., Abstract 979, ICHEP, Amsterdam, July 24–31, 2002, available from `http://www.ichep02.nl/Paper/ABS979.39tAi5.ps`.